Commun. Theor. Phys. **65** (2016) 99–104 Vol. 65, No. 1, January 1, 2016

Electrical Investigation of Armchair Graphene-Graphdiyne-Graphene Nanoribbons Heterojunctions

B. Ghanbari Shohany, M.R. Roknabadi,* and A. Kompany

Department of Physics, Ferdowsi University of Mashhad, Mashhad, Iran

(Received April 27, 2015; revised manuscript received July 7, 2015)

Abstract *In this study, the structural and electronic properties of armchair graphdiyne nanoribbons, which have different widths are studied using the first principle calculation. The results indicate that all studied AGDYNRs show semiconducting behavior in which the band gap values decrease with the increase of nanoribbons width. The electronic and electrical properties of the graphdiyne sandwiched between two graphene nanoribbons are also investigated. The findings of our study indicate that among 4 investigated n-G-GDY-G-NR structures, the highest current is calculated for $n = 3$ (3-G-GDY-G-NR), due to phase transition.*

PACS numbers: 73.63.Rt
Key words: armchair graphdiyne nanoribbon, electrical properties, DFT, NEGF

1 Introduction

Carbon is a unique element in its ability to form the most allotropes in nature.[1] It has been suggested as a promising candidate for use in next generation of electronic and optoelectronic devices. Since, ordinary carbon-based structures such as diamond, graphite and graphene are not semiconductors; therefore many efforts have been devoted to find new carbon-based structures and investigate their electrical properties. Graphdiyne (GDY) was predicted to be semiconductor, around 20 years ago.[2] It is believed that graphdiyne with tunable structural and electronic properties could be applied in fabrication of transistors and other electronic devices.[3−4] As shown in Fig. 1, graphdiyne is a two-dimensional structure possessing both sp and sp^2-hybridized carbon atoms. The presence of the diacetylenic linkages introduces a wide variety of electronic and transport properties.[5]

In order to build graphdiyne-based devices, theoretical research on the band gap modulation of graphdiyne can be helpful to the related experimental studies.[3] In comparison with graphene, GDY has numerous interesting properties, such as high pi-conjunction, uniformly distributed pores, much smaller density, tunable electronic properties, extreme hardness, high thermal resistance and electrical conductivity, which could be attributed to both sp and sp^2-hybridized carbon atoms and its natural holes.[4,6−7] The electronic structure of graphdiyne has been studied by researchers using different computational approaches. It has been concluded that graphdiyne behaves as a semiconductor with a direct band gap at Γ point in a range of 0.46 eV to 1.22 eV, depending on the applied method and the exchange-correlation functional.[7]

After successful synthesis of graphdiyne by Li *et al.*,[8] the electrical, mechanical, optical and magnetic properties of graphdiyne-based nanostructures have been studied, mostly theoretically.[6,9−11] For example, Li *et al.* showed that GDYNRs are stable at room temperature and the carrier concentration of Au- and Cu-decorated 4-AGDNR with 0.5% doping ratio is close to the carrier concentration of the graphene.[3] Pan *et al.* demonstrated that the band gaps of graphyne and graphdiyne nanoribbons decrease as the width of the nanoribbons increase. Also, they showed that these nanoribbons exhibit semiconducting behaviour with the band gaps in the range of 0.54 eV–0.97 eV for armchair and 0.7 eV–1.65 eV for zigzag GDYNRs.[9] Furthermore, the band gap of graphdiyne nanoribbons can be controlled by either ribbon width or electric field.[12] The results of Kang *et al.* indicated that the band gap value decreases by increasing the field strength and a semiconductor-metal transition would occur below a threshold value.[11] In addition, the applications of graphdiyne for energy storage,[13−14] and its use as anode material in batteries[15] have also been reported. Despite several works already performed, still more studies on the electrical properties of graphdiyne are needed.[10]

Up to now, structural,[16−20] electronic,[3,9,21−25] optical,[26] mechanical[10,27−31] and magnetic[6] properties of graphdiyne family have been studied. To our knowledge, very little research has been done to investigate the electrical transport properties of graphdiyne nanoribbons The electrical properties of graphdiyne are of considerable interest, particularly because of the electron transport properties, which may be useful in creating higher performance transistors than are currently available. Therefore, this paper investigates electrical properties of arm-

*E-mail: roknabad@um.ac.ir

chair graphene-graphdiyne-graphene nanoribbons heterojunctions (G-GDY-G-NRs). In this study, first-principle calculations are applied to determine the electronic properties of armchair graphdiyne (AGDYNRs) and armchair graphene-graphdiyne-graphene nanoribbons (G-GDY-G-NRs) with different widths. The effect of width on the electronic and electrical properties is also determined. The results confirmed that the band gap of graphdiyne is adjustable by changing the width of nanoribbons

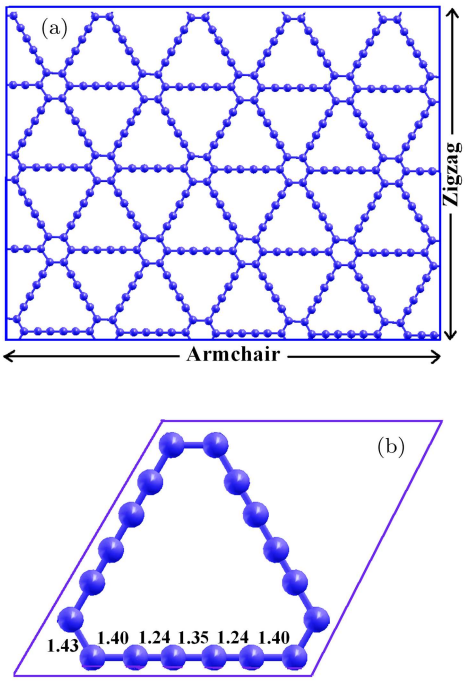

Fig. 1 Structure of graphdiyne sheet (a) and its unit cell (b).

2 Computational Method

Investigation of the atomic structure and electronic properties of graphdiyne nanoribbons were performed using density functional theory (DFT) calculations via SIESTA package, based on localized linear combination of numerical atomic-orbital (LCAO). The generalized gradient approximation (GGA) of Perdew–Burke–Ernzerhof (PBE) for the exchange-correlation functional was used for the electron–electron interactions. The k-grid sampling of $1 \times 1 \times 5$ for the graphdiyne nanoribbons, together with a mesh cutoff of 200 Ry were used in the calculation. A vacuum layer of 20 Å was used for structure optimization and for energy band calculation. Only the armchair nanoribbons ($n = 1, 2, 3, 4$) with diacetylene terminations were investigated. The dangling bonds at the edges were saturated with hydrogen. Then, all these armchair nanoribbons with different widths were optimized until the total atomic forces were converged to less than 0.01 eV/Å.

For electrical properties, calculations were carried out via the non-equilibrium Green's function method [NEGF] as implemented in the TranMain code of OpenMX package. For a bias voltage applied on the system, the current was calculated from the corresponding Green's function and the self-energy by Landauer–Buttiker formula:[32]

$$I(V) = \frac{e}{\hbar} \int_{-\infty}^{+\infty} \{T(E,V)[f_L(E,V) - f_R(E,V)]\} \mathrm{d}E \,,$$

where $T(E,V)$ is the transmission coefficient at energy E and under bias voltage V. f_L and f_R are the Fermi–Dirac distribution functions of the left and right electrodes, respectively.[3,33]

3 Results and Discussion

3.1 *Structural and Electronic Properties*

Figure 2 shows the configurations of 1–4 armchair graphdiyne nanoribbons used in this study. The results reveal that the lattice constant is $a = 9.49$ Å, which is consistent with the previous studies.[7,17–21] C-C bond lengths in hexagons (C6) and in diacetylenic linkages are not equal, implying that C–C hybridization in C links of graphdiyne are different. This difference leads to the greater structural flexibility of GDYs in comparison with graphene.[7] The optimized bond lengths of AGDYNRs are given in Table 1.

Table 1 The optimized bond lengths of armchair graphdiyne nanoribbons.

Bonds type	Optimized lengths/Å
$=C=C=$	1.43
$=C-C=$	1.40
$-C\equiv C-$	1.24
$\equiv C-C\equiv$	1.35

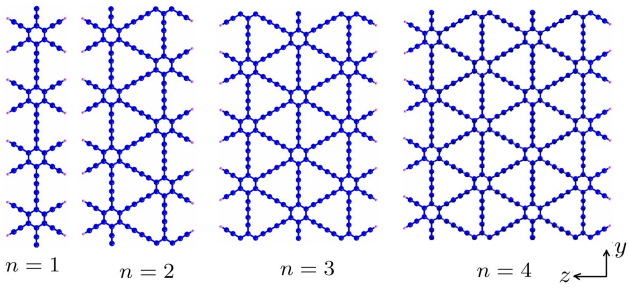

Fig. 2 (Color online) Structure of armchair graphdiyne nanoribbons (blue color) saturated via hydrogen (pink color) after optimization.

The energy band gap of 1-4-AGDYNRs and the total density of states (DOS) are plotted in Fig. 3. It can be seen that Fermi level is chosen as zero point. AGDYNRs are semiconductors with direct transition at the Γ and X points of the first Brillouin zone. The obtained band gaps

of 1-4-AGDYNRs are 1.2 eV, 0.9 eV, 0.75 eV, 0.7 eV, respectively. The gap of AGDYNRs occurs at Γ point in the first Brillouin zone, so this gap is mainly affected by the states adjacent to Γ point, which are not located close to the boundary states in the Brillouin zone. The localized states are appeared in 1-AGDYNR due to quantum confinement and edge effect. As it can be observed in Fig. 3, the band structure and DOS curves match with each other. Also the density of states (DOS) at the Fermi level is zero, showing the semiconducting behavior of the nanoribbons. DFT calculations reveal that the density of electronic states around the Fermi level increases with increasing the width of the nanoribbon.

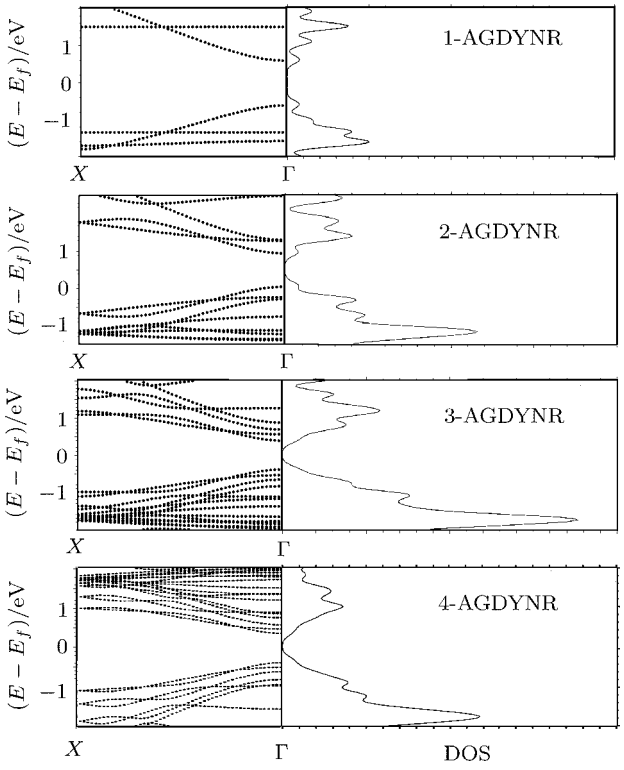

Fig. 3 The energy bands and total density of states (DOS) of armchair graphdiyne nanoribbons.

As shown in Fig. 4, due to the quantum confinement effect, the band gap of AGDNRs is clearly width dependent and decreases as the width of graphdiyne increases. This result is consistent with some other reports.[9]

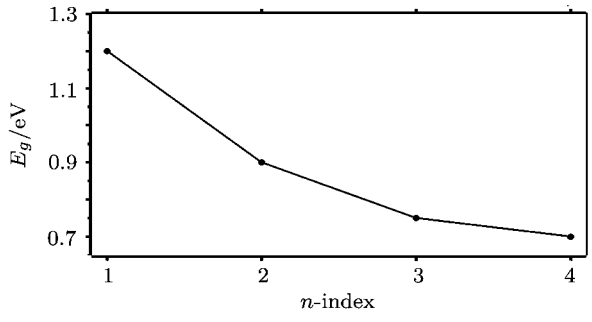

Fig. 4 Variation of band gap energy (eV) versus n-index for armchair graphdiyne nanoribbons.

For further investigation of the bonding types, the density of states was projected onto the atomic orbitals (P_x, P_y, P_z). Figure 5 depicts the PDOS of armchair graphdiyne nanoribbons. The electronic states near the Fermi level are contributed by P_z orbital, therefore the bonding is mainly π type. The spectra of graphdiyne includes deeply located σ-type bands, while the low-energy $\pi(\pi^*)$ bands form the edges of the gap. These results are in agreement with the previous calculations.[3,7,9]

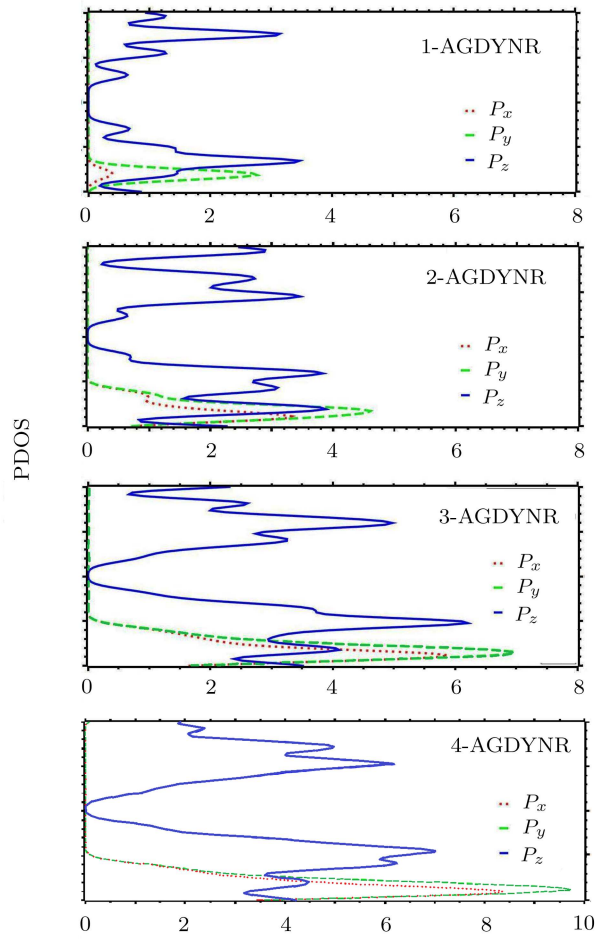

Fig. 5 Projected density of states (PDOS) of armchair graphdiyne nanoribbons.

The heterojunctions of armchair graphene-graphdiyne-graphene nanoribbons, as shown for 1-G-GDY-G-NR in Fig. 6, were constructed and relaxed. The electronic band structures of 1-4 armchair graphene-graphdiyne-graphene nanoribbons are plotted in Fig. 7. The Fermi energy is taken as zero point. For 1-4-G-GDY-G nanoribbons, band gap oscillations are found as a function of the nanoribbon width, similar to graphene nanoribbons.[34] The gap value becomes smaller as the ribbon width increases until the valence and conduction bands overlap at the Fermi level in 3-G-GDY-G ribbon, and then with increasing the width to $n = 4$, the gap appears again.

As a result, band gaps in n-AGDYNRs would be larger than those in n-G-GDY-G-NRs with similar n.

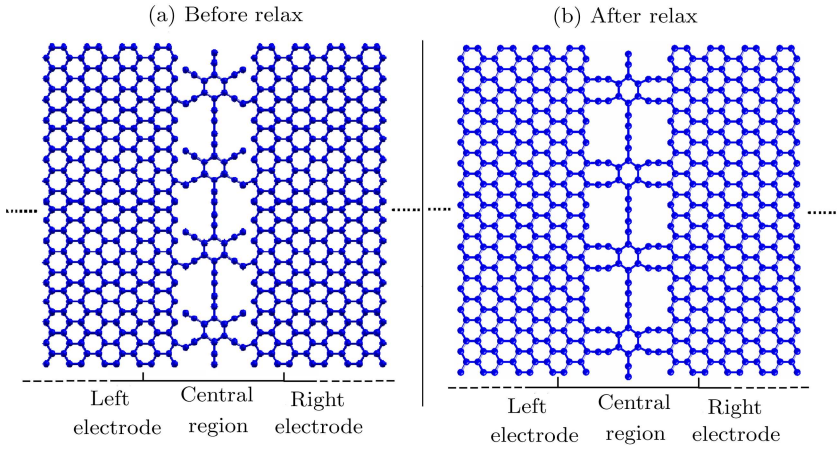

Fig. 6 Structure of $n = 1$ armchair graphene-graphdiyne-graphene heterojunctions (a) before (b) after optimization.

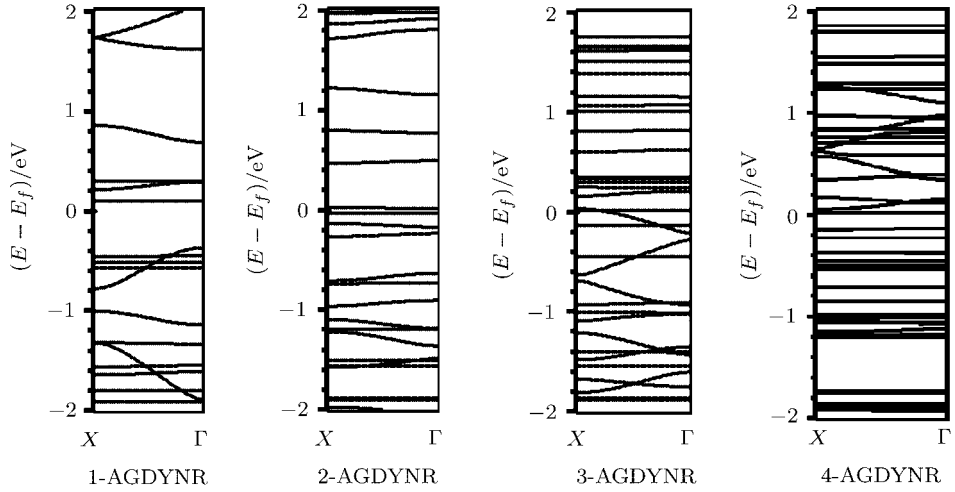

Fig. 7 The electronic band structures of armchair graphene-graphdiyne-graphene nanoribbons.

3.2 *Electrical Properties*

For manufacturing electronic devices such as field effect transistor (FET), the electrical investigation of armchair graphene-graphdiyne-graphene nanoribbons is needed. A study of the conductance through a pristine nanoribbon within the framework of the Landauer formalism is presented in this section. The transport properties are obtained using the NEGF method, where the Hamiltonian matrix is generated through DFT. For the electron transport, the TranMain code of Open MX package is used. As shown in Fig. 6, the system is divided in three parts: left electrode, central region, and right electrode. It is assumed that the electrodes coupled only with the central region.

Figure 8 illustrates the calculated current of G-GDY-G-NRs at bias voltages in the range of zero to 2 V. As the Fig. 8 shows, below a threshold voltage the current is almost zero and for higher voltages it remarkably increases. The obtained results indicate that the current decreases by increasing the width of the nanoribbons, due to the increase of electron scattering. But 3-G-GDY-G-NR shows the highest current because of phase transition. This result is in agreement with the oscillation of band gap.

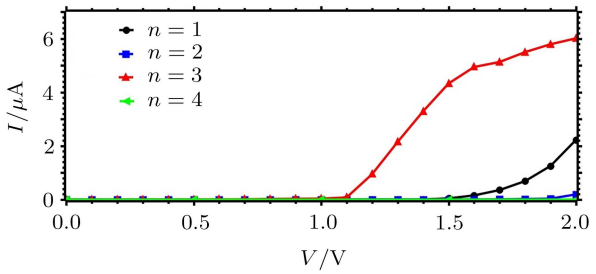

Fig. 8 I-V curve of armchair graphene-graphdiyne-graphene heterojunctions.

For better understanding the behavior of I–V characteristic, the transmission curves are presented for the 1-G-

GDY-G-NRs at $V = 0$ V, 1 V, 2 V in Fig. 9. By increasing the applied voltage, the bias window $[-eV/2, +eV/2]$ is opened and different transmission peaks contribute in the transport of 1-G-GDY-G-NRs. With an increase in the applied voltage, the valence band (π band) in the left electrode overlaps with the conduction band (π^* band) in the right electrode within the bias window. So the electrons in the valence band of the left electrode are allowed to be transmitted to the conduction band of the right one. Thus transmission peaks arise around the Fermi level, as can be seen in Fig. 9. The transmission coefficient in the bias window increases by increasing the bias voltage. As a result, the current, that is determined by the integral of $T(E, V)$ over the bias window, increases.[35−36]

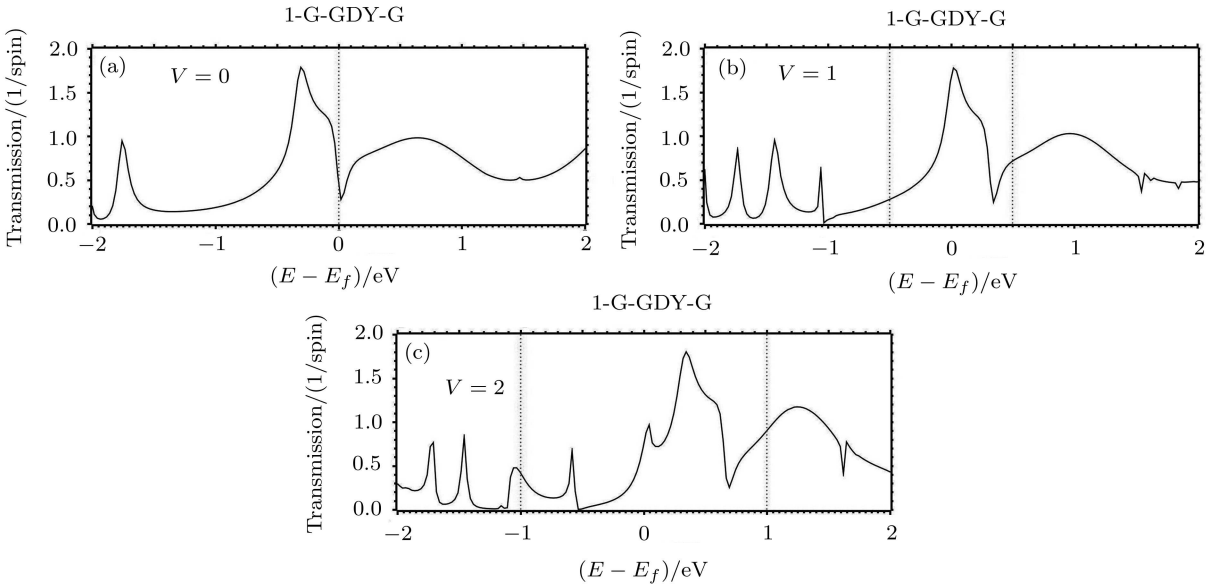

Fig. 9 Transmission spectra of 1-G-GDY-G-NR at different bias voltages.

4 Conclusion

In summary, via *ab initio* study, it is shown that armchair graphdiyne nanoribbons possess notable structural, electronic and electrical properties. The lengths of C-C bonds are not equal; therefore graphdiyne has greater structural flexibility in comparison with graphene. Regarding the electronic properties, all studied graphdiyne nanoribbons are semiconductors with the tunable direct band gap at Γ point. Due to the quantum confinement and edge effect, the band gap of studied AGDNRs decreases as the width of graphdiyne increases. The projected density of state shows that the electronic states near the Fermi level are contributed by P_z orbital and therefore the bonding is mainly π type. In addition, the results showed that the electrical transport properties of the armchair graphene-graphdiyne-graphene nanoribbons are affected by the width of nanoribbons. By increasing the width, the current decreases because of increase of electron scattering, but the G-GDY-G-NR with $n = 3$ has the highest current, in comparison with $n = 1, 2, 4$, due to phase transition.

References

[1] A. Wang, L. Li, X. Wang, H. Bu, and M. Zhao, Diam. Relat. Mater. **41** (2014) 65.

[2] C.S. Ozkan, M.J. Buehler, N.M. Pugno, and K. Wang, J. Mater. Res. **28** (2013) 909.

[3] Z. Lin, Q. Wei, and X. Zhu, Carbon **66** (2014) 504.

[4] Q. Zheng, G. Luo, Q. Liu, R. Quhe, J. Zheng, K. Tang, Z. Gao, S. Nagase, and J. Lu, Nanoscale **4** (2012) 3990.

[5] S.W. Cranford and M.J. Buehler, Nanoscale **4** (2012) 4587.

[6] J. He, S.Y. Ma, P. Zhou, C.X. Zhang, C. He, and L.Z. Sun, J. Phys. Chem. C **116** (2012) 26313.

[7] A.L. Ivanovskii, Prog. Solid State Chem. **41** (2013) 1.

[8] G. Li, Y. Li, H. Liu, Y. Guo, Y. Li, and D. Zhu, Chem. Commun. **46** (2010) 3256.

[9] L.D. Pan, L.Z. Zhang, B.Q. Song, S.X. Du, and H.J. Gao, Appl. Phys. Lett. **98** (2011) 173102.

[10] Y. Pei, Physica B **407** (2012) 4436.

[11] J. Kang, F. Wu, and J. Li, J. Phys. Condens. Matter **24** (2012) 165301.

[12] Q. Peng, A.K. Dearden, J. Crean, L. Han, S. Liu, X. Wen, and S. De, Nanotechnol. Sci. Appl. **7** (2014) 1

[13] Y. Jiao, A. Du, M. Hankel, Z. Zhu, V. Rudolph, and S.C. Smit, Chem. Commun. **47** (2011) 11843.

[14] J. Drogar, M.R. Roknabadi, M. Behdani, M. Modarresi, and A. Kari, Superlattice Microst. **75** (2014) 340.

[15] K. Srinivasu and S.K. Ghosh, J. Phys. Chem. C **116** (2012) 5951.

[16] H. Bu, M. Zhao, H. Zhang, X. Wang, Y. Xi, and Z. Wang, J. Phys. Chem. A **116** (2012) 3934.

[17] N. Narita, S. Nagai, S. Suzuki, and K. Nakao, Phys. Rev. B **58** (1998) 11009.

[18] R.C. Andrew, R.E. Mapasha, A.M. Ukpong, and N. Chetty, Phys. Rev. B **85** (2012) 125428.

[19] H. Bai, Y. Zhu, and W. Qiao, R. Soc. Chem. Adv. **1** (2011) 768.

[20] M. Long, L. Tang, D. Wang, Y. Li, and Z. Shuai, ACS Nano **5** (2011) 2593.

[21] D. Malko, C. Neiss, and A. Gorling, Phys. Rev. B **86** (2012) 45443.

[22] H.J. Cui, X.L. Sheng, Q.B. Yan, Q.R. Zheng, and G. Su, arXiv:1211.3188.

[23] S.W. Cranford and M.J. Buehler, Carbon **49** (2011) 4111.

[24] J. Kang, J. Li, F. Wu, S.S. Li, and J.B. Xia, J. Phys. Chem. C **115** (2011) 20466.

[25] A.N. Enyashin and A.L. Ivanovskii, Phys. Status Solidi B **248** (2011) 1879.

[26] G. Luo, Q. Zheng, W.N. Mei, J. Lu, and S. Nagase, J. Phys. Chem. C **117** (2013) 13072.

[27] Y. Yang and X. Xu, Comp. Mater Sci. **61** (2012) 83.

[28] Y.Y. Zhang, Q.X. Pei, and C.M. Wang, Appl. Phys. Lett. **101** (2012) 81909.

[29] M. Mirnezhad, R. Ansari, H. Rouhi, M. Seifi, and M. Faghihnasiri, Solid State Commun. **152** (2012) 1885.

[30] A. Bosak, M. Krisch, M. Mohr, J. Maultzsch, and C. Thomsen, Phys. Rev. B **75** (2007) 153408

[31] K.N. Kudin, G.E. Scuseria, and B.I. Yakobson, Phys. Rev. B **64** (2001) 235406

[32] Z. Sohbatzadeh, M.R. Roknabadi, N. Shahtahmasebi, and M. Behdani, Physica E **65** (2015) 61.

[33] Y. Jing, G. Wu, L. Guo, Y. Sun, and J. Shen, Computational Materials Science **78** (2013) 22.

[34] Z. Jiang and Y. Song, Physica B **464** (2015) 61.

[35] W.K. Zhao, G.M. Ji, and D.S. Liu, Phys. Lett. A **378** (2014) 446.

[36] W. Wu, W. Guo, and X.C. Zeng, Nanoscale **5** (2013) 9264.